

A.1 Groundwater Well Data

Groundwater elevation measurements collected in the spring were evaluated as a potential predictor of river flow behavior the following fall. The length of the records and number of spring-season measurements were variable, limiting the number of wells that could be used as predictor sites. Two wells were selected for the final predictor evaluation.

Correlation coefficients between April groundwater elevations and subsequent September flow volume

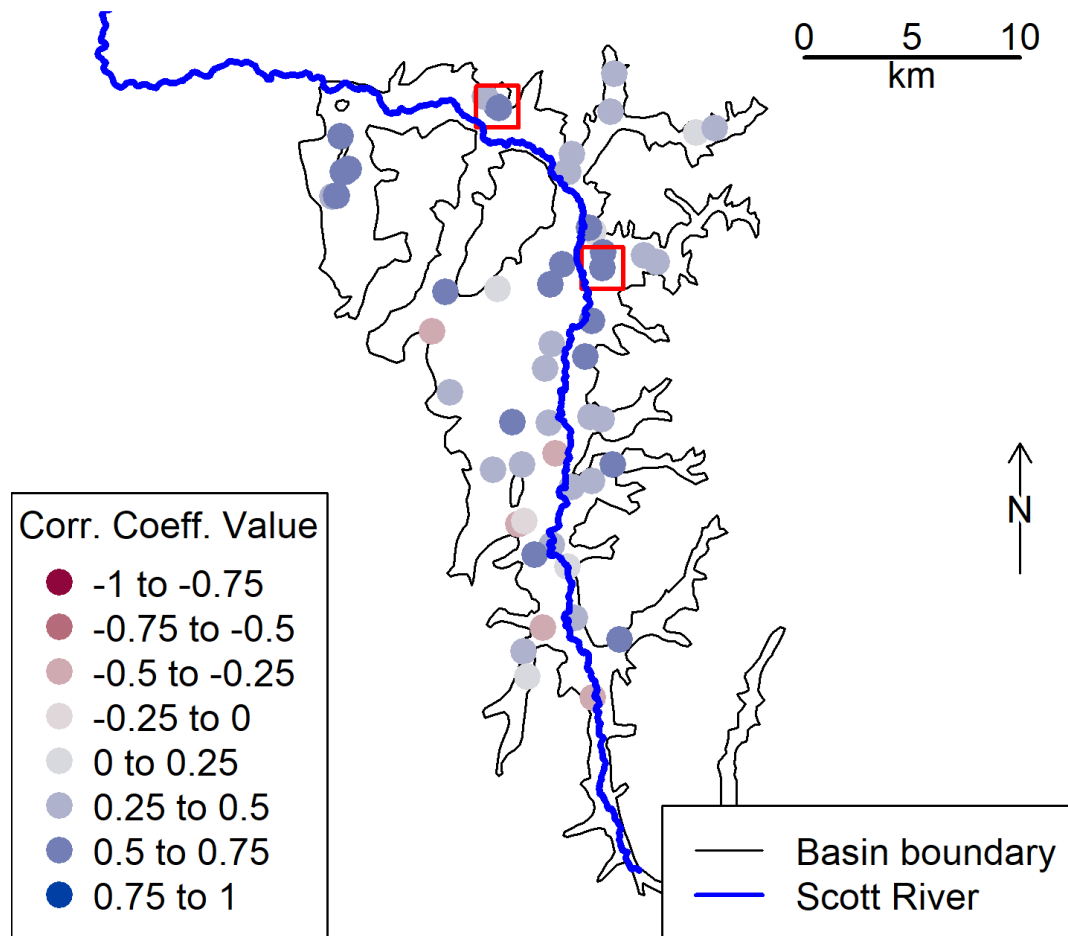


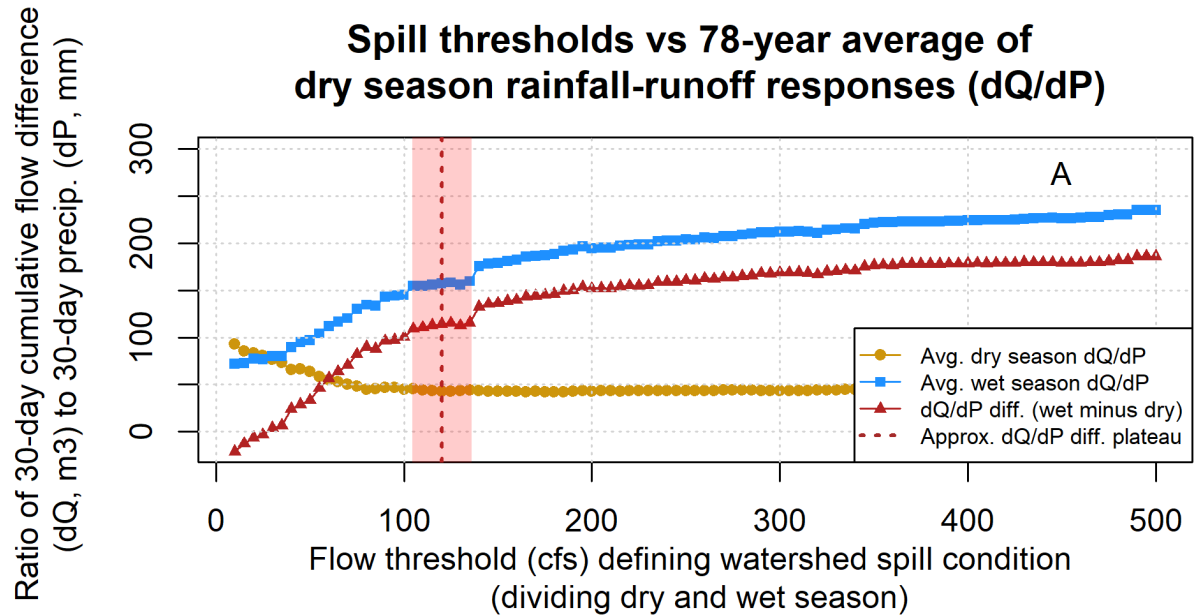
Figure A1. Boundary of the groundwater basin (corresponding approximately to the extent of the flat valley floor in the Scott River watershed) and selected well locations. Colors correspond to the correlation coefficients between April groundwater elevations and September flow volume. The wells included in the predictor comparison are highlighted with a red outer square. 54 wells had enough spring-season water level measurements to be included in this correlation exercise, though some wells are so close together that their symbols overplot on this map.

530 A.2 Selection of the Q_{spill} threshold value

The Q_{spill} value of 120 cfs (294 thousand m^3/day or approximately 9 Mm^3 per month) was determined by testing a range of potential Q_{spill} values (10 to 500 cfs [24 to 1223 thousand m^3/day]) as a dividing threshold between dry- and wet-season flow behavior. Specifically, the threshold, Q_{spill} , was here operationally defined as the flow rate that generated the largest, difference in rainfall-runoff response on either side of the dry season-wet season divide (Figure A2, Panel A). The rainfall-runoff response was measured as the ratio dQ/dP , where dQ is the change in runoff and dP is the cumulative precipitation over the same moving 30-day period. Hence, the objective of this analysis was to find Q_{spill} such that the difference between the two dQ/dP values for the 30 days immediately prior to reaching Q_{spill} and the 30 days immediately following the day when Q_{spill} reaches an initial maximum.

For the Scott Valley watershed, the difference between the wet and dry season rainfall-runoff responses reaches an initial plateau (113 cfs [275 m^3/day] of increased flow per mm of precipitation) for spill thresholds from 105-135 cfs (256-330 $10^3 m^3/day$) (Figure A2, Panel A). This indicates that in a large number of water years, flows in the range of 105-135 cfs (257 to 330 thousand m^3/day) range are preceded by a dry season flow-response regime and followed by a distinct, flashier flow regime regime. Though higher wet-dry flow response differences were calculated at higher threshold values (i.e., up to 500 cfs [1,223 thousand m^3/day]), these progressively higher wet-season flow responses likely reflect the falling limb of individual large storms that over-fill the watershed rather than separating filling from spilling behavior.

Additionally, in visual inspection of 78 years of Fort Jones hydrographs, the 120 cfs (294 $10^3 m^3/day$) Q_{spill} threshold generated a plausible breakpoint between dry and wet season river behavior in all water years (e.g., water year 2018 in Figure A2, Panel B). Furthermore, this value corroborates local observations that an approximate value of 100 cfs represents “fully connected” river conditions (see Discussion section).



Fort Jones Gauge Flow and Cum. Precip., 2015-2016

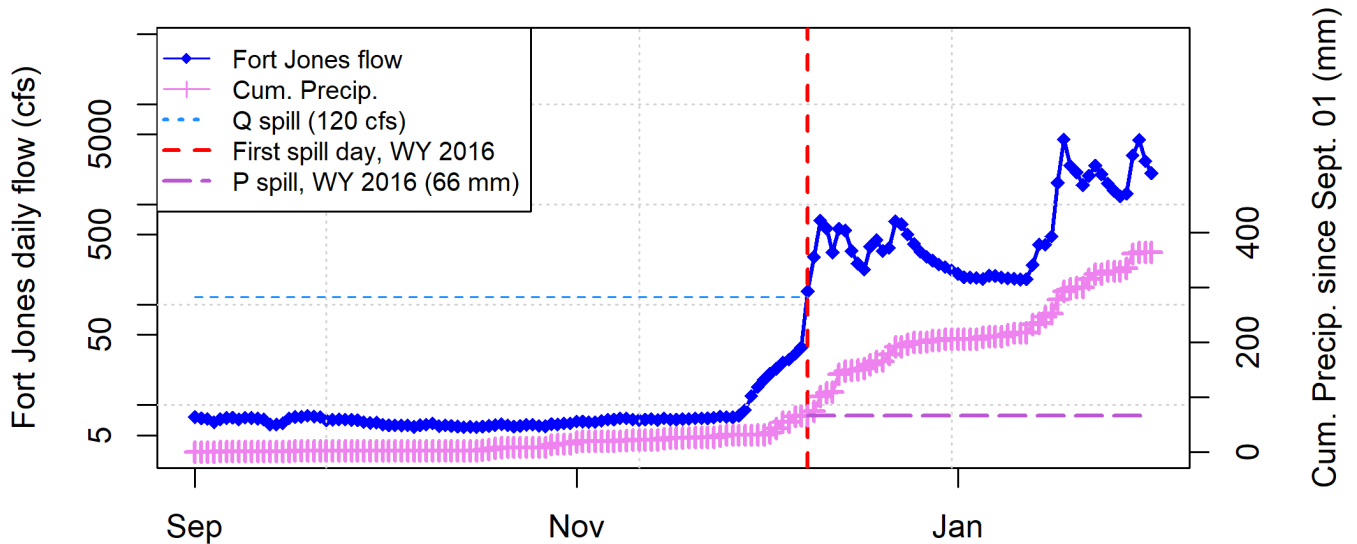


Figure A2. This analysis (Panel A) aimed to identify the flow threshold that approximately defines the boundary between filling (i.e. dry season) and spilling (i.e. wet season) flow behavior at the Fort Jones gauge. For each threshold value, for each water year, a rainfall-runoff response was calculated before and after the flow threshold. The rainfall-runoff response consisted of the 30-day cumulative flow difference (dQ) per 30-day cumulative rainfall difference (dP). 120 cfs was selected as the threshold value dividing the dry and wet seasons (e.g., Panel B).

Diagnostics used to select the predictive models for V_{min} are shown below and discussed in Results. Predictors are abbreviated in tables and described briefly in Table A1; for more information on potential predictors see Section 2.3.

Table A1. Linear model diagnostics for one-predictor models of minimum fall flows (V min).

Predictor ID	Predictor Descrip.	n	Log Likelihood	AIC	LOOCV	R squared
SWJ_max_wc_mm	Snow maximum	70	-131	269	2.7	0.53
USC00043182_oct_apr_mm	Oct.-Apr. Precip.	75	-142	290	2.7	0.49
SWJ_jday_of_max	Snow maximum timing	70	-154	314	5.1	0.11
springWL_415635N1228315W001	March-May WLs	50	-100	206	3.6	0.39
et0_oct_apr	ET Ref.	17	-21	48	0.9	0.46
mar_flow	March flow vol.	78	-162	330	4.1	0.25

Table A2. Linear model diagnostics for two-predictor models of V min. See table of one-predictor models for description of predictor IDs. Reference ET was not included in two- and three-predictor models due to an insufficient sample size.

Predictor 1	Predictor 2	n	Log Likelihood	AIC	LOOCV	R squared
SWJ_max_wc_mm	USC00043182_oct_apr_mm	67	-119	246	2.3	0.62
SWJ_max_wc_mm	SWJ_jday_of_max	70	-131	270	2.8	0.53
SWJ_max_wc_mm	springWL_415635N1228315W001	50	-91	191	2.7	0.57
SWJ_max_wc_mm	mar_flow	70	-128	264	2.6	0.57
USC00043182_oct_apr_mm	SWJ_jday_of_max	67	-127	263	2.9	0.52
USC00043182_oct_apr_mm	springWL_415635N1228315W001	47	-91	190	3.3	0.48
USC00043182_oct_apr_mm	mar_flow	75	-139	286	2.8	0.52
SWJ_jday_of_max	springWL_415635N1228315W001	50	-97	203	3.3	0.45
SWJ_jday_of_max	mar_flow	70	-141	291	3.8	0.37
springWL_415635N1228315W001	mar_flow	50	-94	197	3.1	0.51

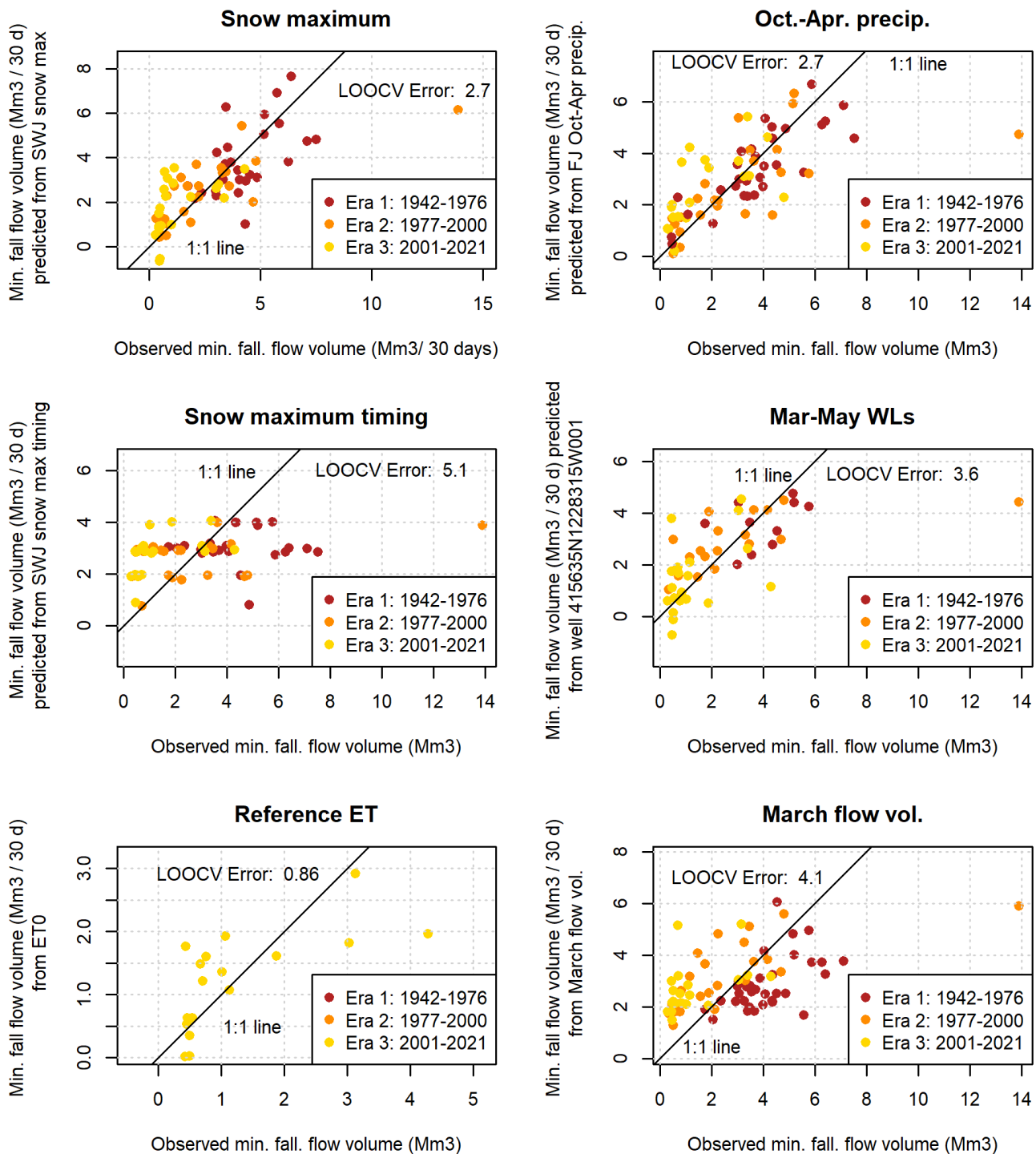


Figure A3. Single-predictor models of minimum 30-day dry season baseflows in the Scott River.

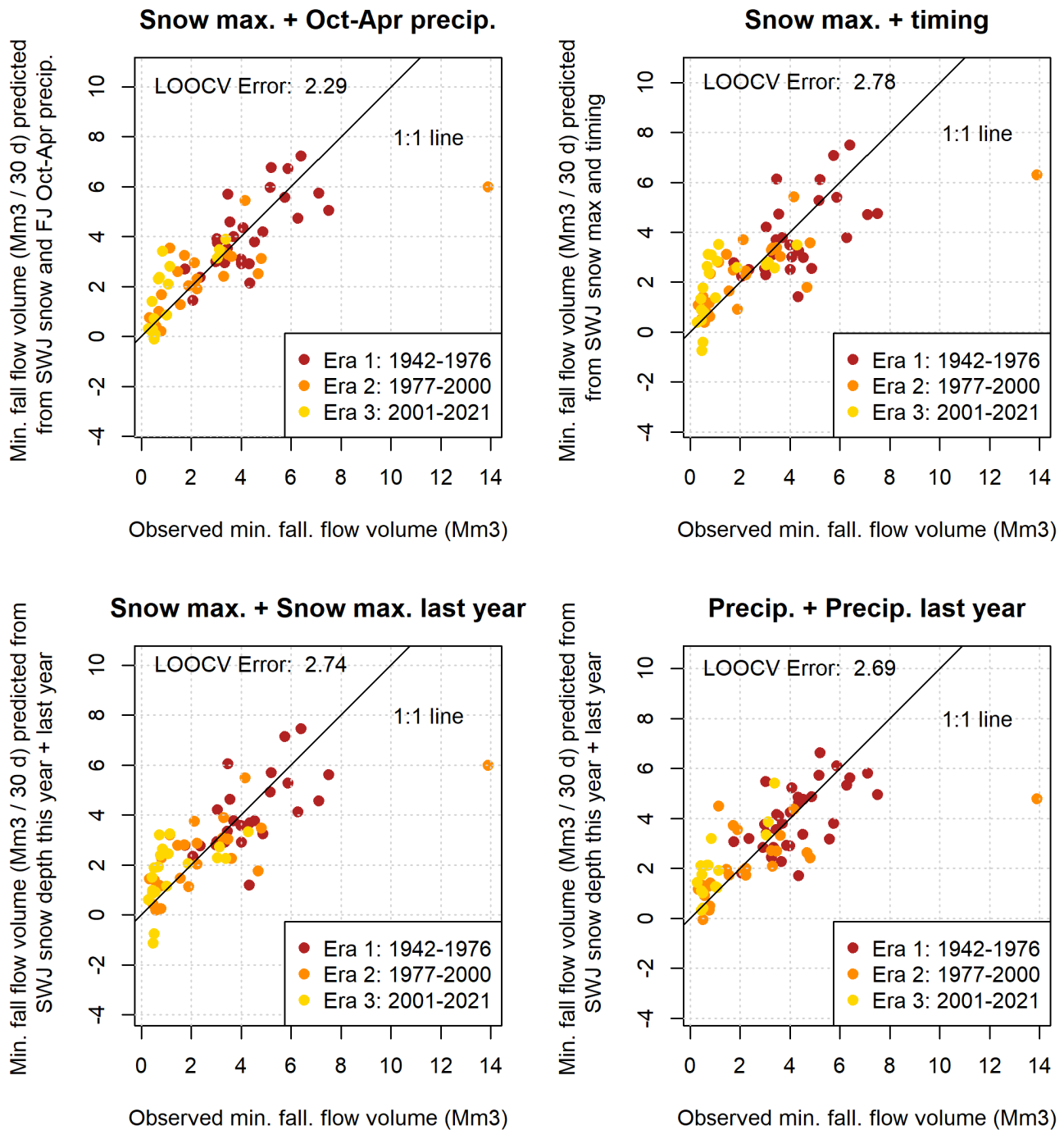


Figure A4. Two-predictor models of minimum 30-day dry season baseflows in the Scott River.

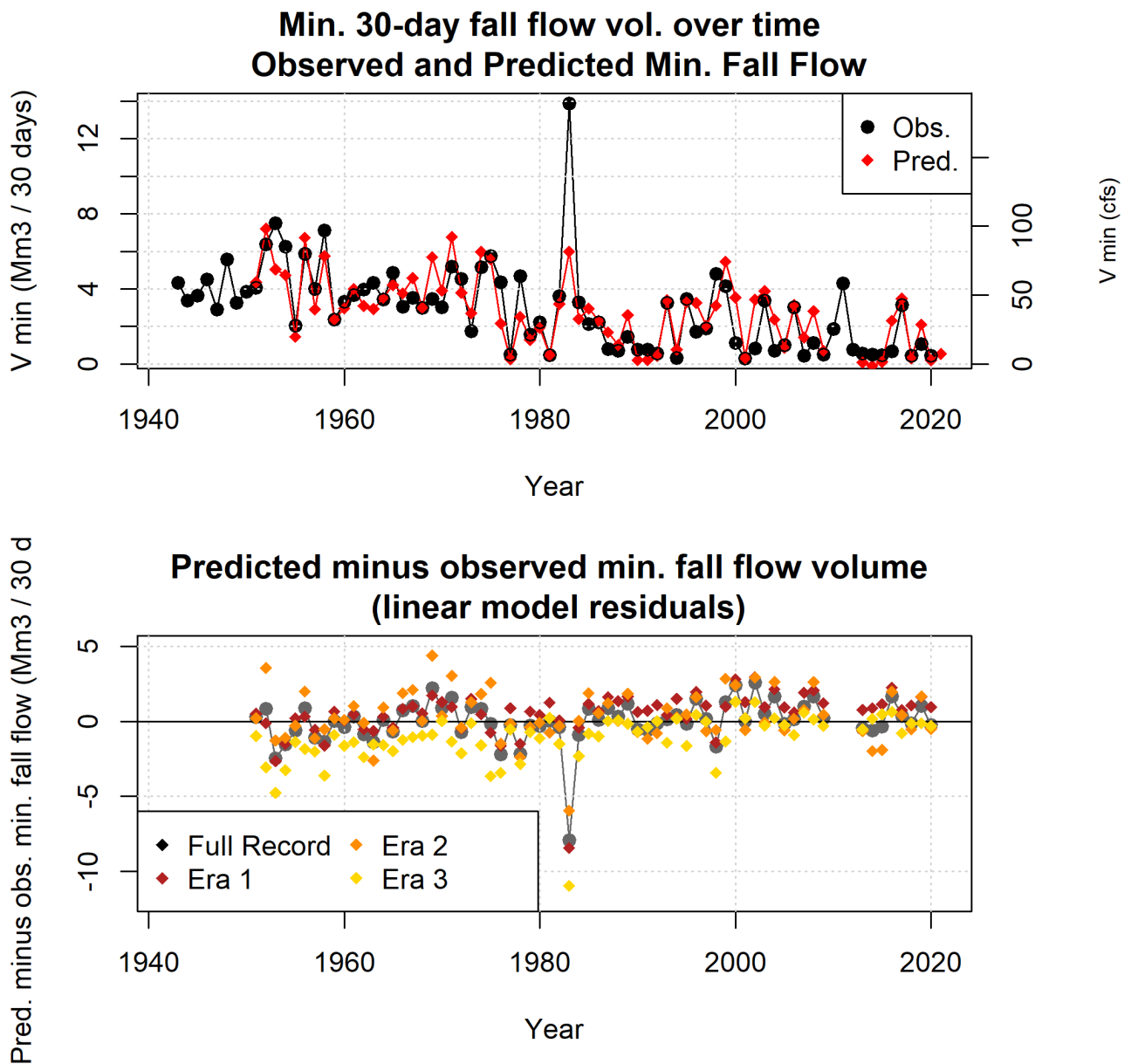


Figure A5. Observed and predicted minimum 30-day dry season baseflows both trend downward between the three eras of the period of record (top panel). The predicted-minus-observed difference (residual) over time also reflects this trend, underpredicting minimum flows pre-1977 and overpredicting them post-2000 (middle panel). The predictive model is based on observations from the full record, but three additional models were generated based on only the observations from Eras 1, 2, and 3. Residuals based on Era 1 data are similar to those of the full record; Era 2 residuals tend to overpredict more than the full record; and Era 3 residuals show better performance post-2000 than the full record, but significant underprediction pre-2000.

Table A3. Linear model diagnostics for three-predictor models of minimum fall flows (V min). See table of one-predictor models for description of predictor IDs. Reference ET was not included in two- and three-predictor models due to an insufficient sample size.

Predictor 1	Predictor 2	Predictor 3	n	Log Like.	AIC	LOOCV	R squared
SWJ_max_wc_mm	USC00043182_oct_apr_mm	SWJ_jday_of_max	67	-119	247	2.3	0.63
SWJ_max_wc_mm	USC00043182_oct_apr_mm	springWL_415635N1228315W001	47	-86	181	2.8	0.59
SWJ_max_wc_mm	USC00043182_oct_apr_mm	mar_flow	67	-117	244	2.3	0.64
SWJ_max_wc_mm	SWJ_jday_of_max	springWL_415635N1228315W001	50	-91	192	2.7	0.58
SWJ_max_wc_mm	SWJ_jday_of_max	mar_flow	70	-127	265	2.7	0.58
SWJ_max_wc_mm	springWL_415635N1228315W001	mar_flow	50	-89	187	2.6	0.61
USC00043182_oct_apr_mm	SWJ_jday_of_max	springWL_415635N1228315W001	47	-90	190	3.3	0.51
USC00043182_oct_apr_mm	SWJ_jday_of_max	mar_flow	67	-123	256	2.8	0.58
USC00043182_oct_apr_mm	springWL_415635N1228315W001	mar_flow	47	-87	184	3.0	0.56
SWJ_jday_of_max	springWL_415635N1228315W001	mar_flow	50	-91	191	2.9	0.58

A.4 Model selection criteria - P_{spill}

555 Diagnostics used to select the predictive models for P_{spill} are shown below and discussed in Results. Predictors are abbreviated in tables and described briefly in Table A4; for more information on potential predictors see Section 2.3.

Table A4. Linear model diagnostics for one-predictor models of P spill.

Predictor ID	Predictor Descrip.	n	Log Likelihood	AIC	LOOCV	R squared
SWJ_max_wc_mm	Snow maximum	70	-333	673	850	0.38
USC00043182_oct_apr_mm	Oct.-Apr. Precip.	75	-351	708	718	0.43
SWJ_jday_of_max	Snow maximum timing	70	-347	699	1243	0.09
springWL_415635N1228315W001	March-May WLs	50	-245	495	1123	0.24
et0_oct_apr	ET Ref.	17	-81	167	932	0.23
mar_flow	March flow vol.	78	-380	767	1061	0.14

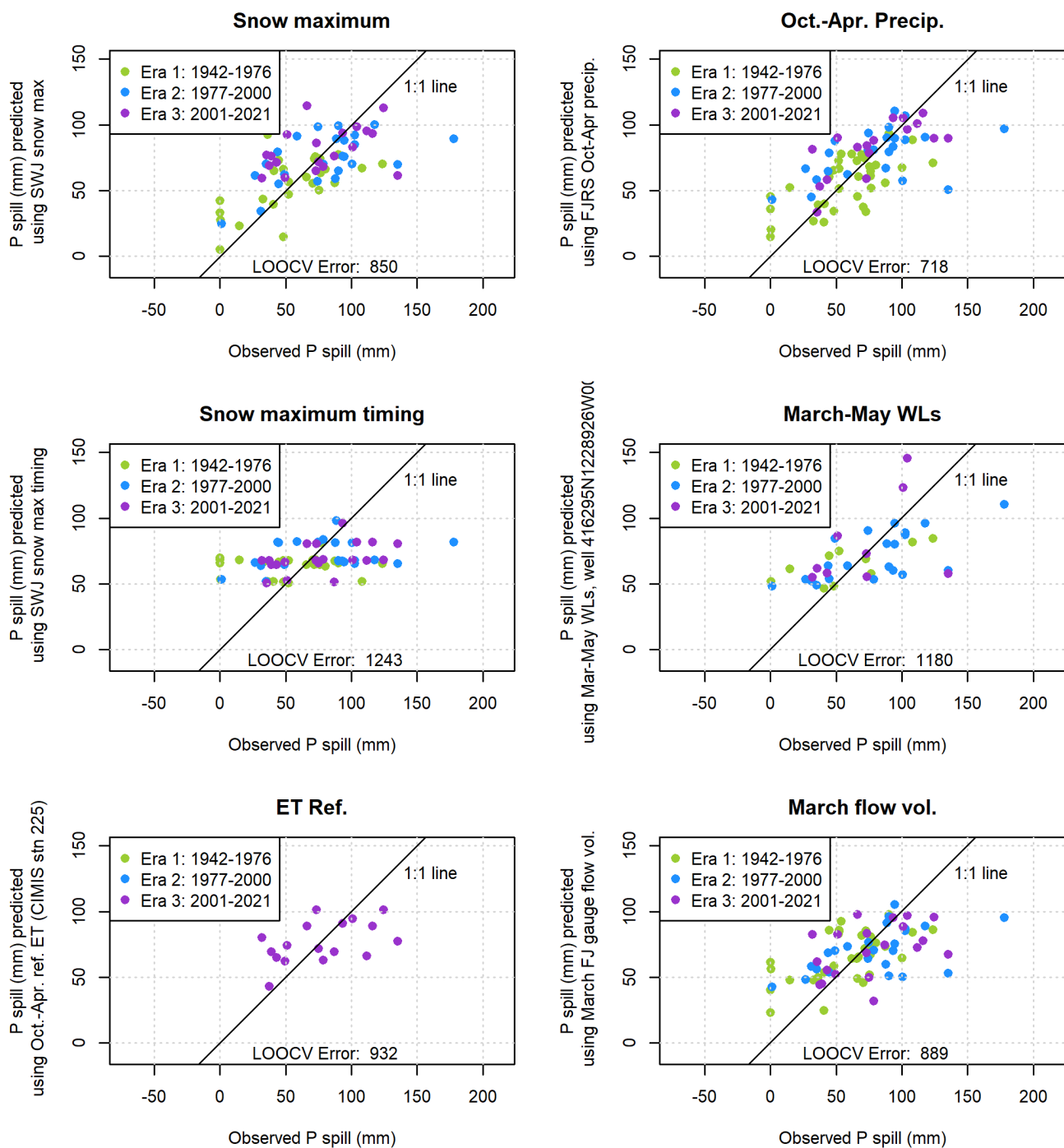


Figure A6. Single-predictor models of P spill, the cumulative precipitation after the dry season needed to generate 120 cfs of flow in the Scott River.

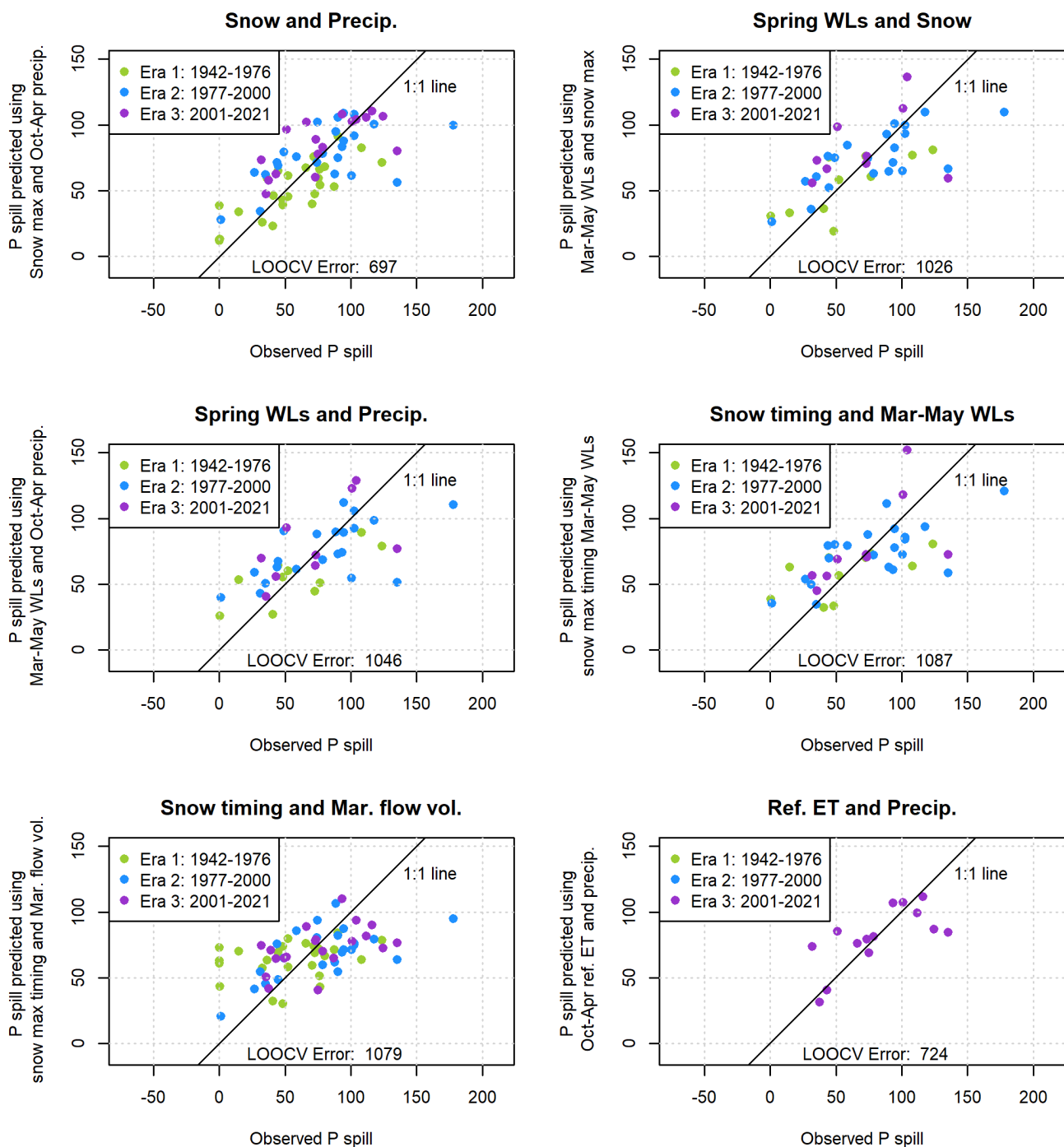


Figure A7. Two-predictor models of P spill, the cumulative precipitation after the dry season needed to generate 120 cfs of flow in the Scott River.

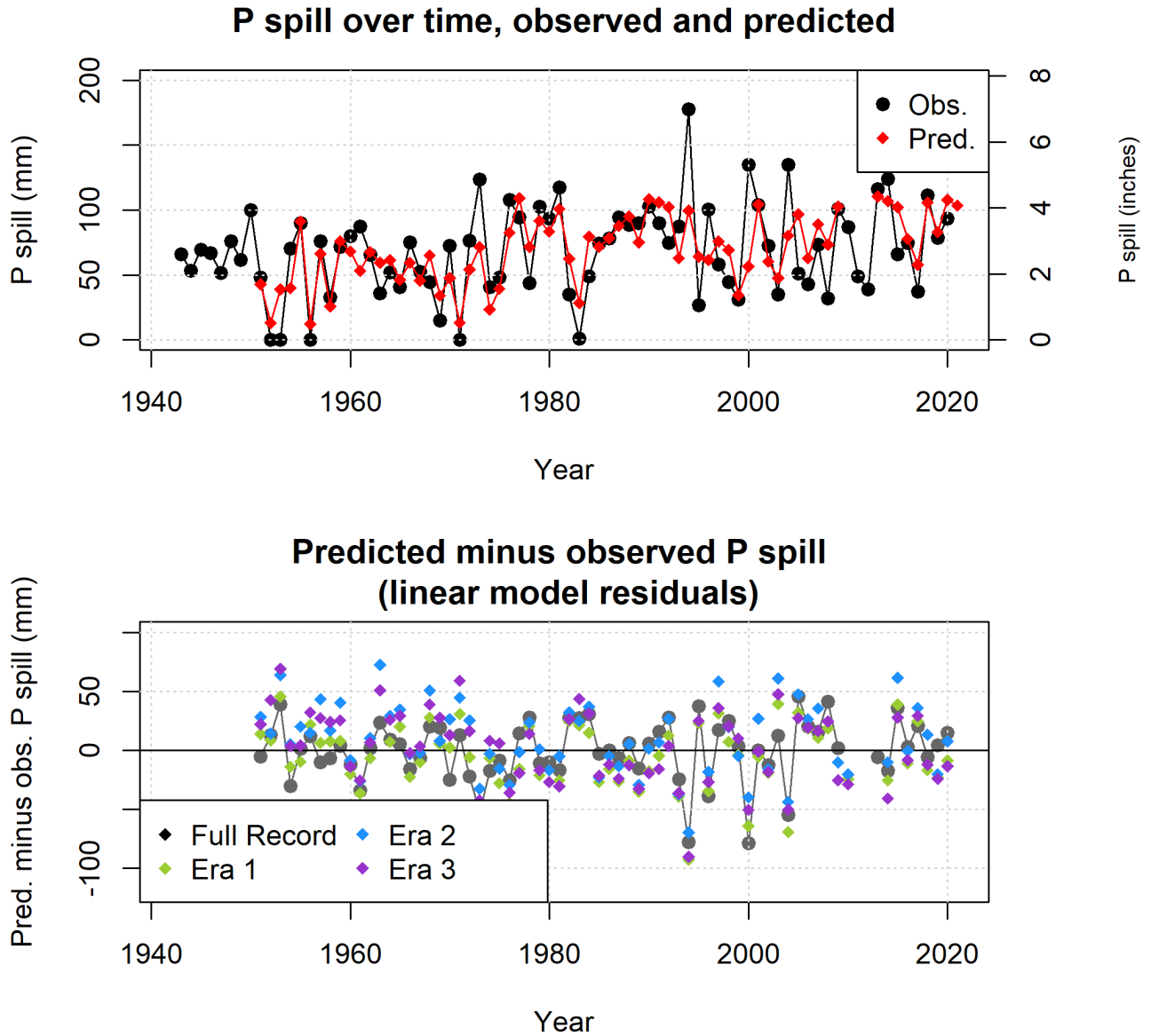


Figure A8. Observed and predicted values of P spill (panel A) indicate a worse model fit for the P spill prediction than for minimum 30-day dry season baseflows. Serious overprediction in Era 1 is followed by more mixed over- and under-prediction in Eras 2 and 3 (bottom panel). The overall P spill model is based on observations from the full record, but three additional models were generated based on only the observations from Eras 1, 2, and 3. Residuals based on Era 1 data are generally lower than those from Eras 2 or 3 or from the full record.

Table A5. Linear model diagnostics for two-predictor models of P spill. See table of one-predictor models for description of predictor IDs. Reference ET was not included in two- and three-predictor models due to an insufficient sample size.

Predictor 1	Predictor 2	n	Log Likelihood	AIC	LOOCV	R squared
SWJ_max_wc_mm	USC00043182_oct_apr_mm	67	-312	631	697	0.51
SWJ_max_wc_mm	SWJ_jday_of_max	70	-333	674	870	0.39
SWJ_max_wc_mm	springWL_415635N1228315W001	50	-240	487	951	0.38
SWJ_max_wc_mm	mar_flow	70	-333	674	853	0.39
USC00043182_oct_apr_mm	SWJ_jday_of_max	67	-315	637	760	0.47
USC00043182_oct_apr_mm	springWL_415635N1228315W001	47	-224	457	920	0.43
USC00043182_oct_apr_mm	mar_flow	75	-351	709	728	0.44
SWJ_jday_of_max	springWL_415635N1228315W001	50	-243	493	1068	0.30
SWJ_jday_of_max	mar_flow	70	-341	690	1079	0.23
springWL_415635N1228315W001	mar_flow	50	-242	493	1067	0.31

Table A6. Linear model diagnostics for three-predictor models of P spill. See table of one-predictor models for description of predictor IDs. Reference ET was not included in two- and three-predictor models due to an insufficient sample size.

Predictor 1	Predictor 2	Predictor 3	n	Log Like.	AIC	LOOCV	R squared
SWJ_max_wc_mm	USC00043182_oct_apr_mm	SWJ_jday_of_max	67	-311	633	712	0.52
SWJ_max_wc_mm	USC00043182_oct_apr_mm	springWL_415635N1228315W001	47	-222	455	874	0.47
SWJ_max_wc_mm	USC00043182_oct_apr_mm	mar_flow	67	-312	633	714	0.51
SWJ_max_wc_mm	SWJ_jday_of_max	springWL_415635N1228315W001	50	-239	488	973	0.39
SWJ_max_wc_mm	SWJ_jday_of_max	mar_flow	70	-332	675	872	0.40
SWJ_max_wc_mm	springWL_415635N1228315W001	mar_flow	50	-239	488	955	0.40
USC00043182_oct_apr_mm	SWJ_jday_of_max	springWL_415635N1228315W001	47	-224	457	936	0.44
USC00043182_oct_apr_mm	SWJ_jday_of_max	mar_flow	67	-314	638	768	0.48
USC00043182_oct_apr_mm	springWL_415635N1228315W001	mar_flow	47	-223	457	923	0.45
SWJ_jday_of_max	springWL_415635N1228315W001	mar_flow	50	-240	490	1008	0.37

A.5 Diagnostic plots for selected models

Standard diagnostic plots for the selected predictive models for V_{min} and P_{spill} . For V_{min} , these diagnostic plots highlight outlier record 42, which corresponds to the year 1983, when an early September storm followed a wet year. For P_{spill} , three lesser outliers are highlighted, corresponding to water years 1994, 2000 and 2004, in which the three highest values of P_{spill} were observed. These outliers represent the basin in extreme hydrologic conditions, so are retained in the dataset even though they exert disproportionate leverage over the predictive models.

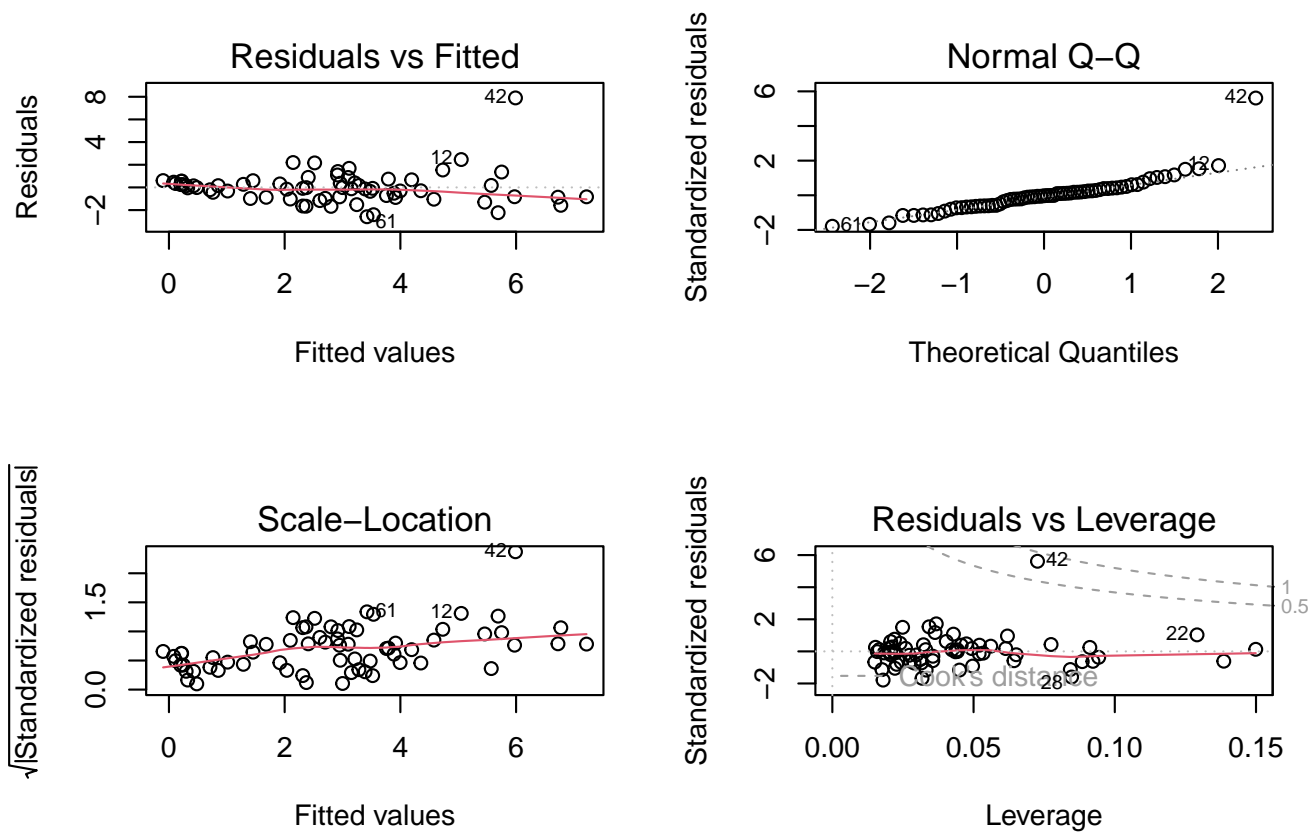


Figure A9. Diagnostic plots for the selected predictive models of V min.

. Analyses and figures in this manuscript were drafted in RMarkdown. The RMarkdown scripts are available on the corresponding author's GitHub page. All data used in this manuscript are publicly available on local, state or federal data portals.

. The authors declare no competing interests.

565 . This manuscript emerged from dissertation work funded by Siskiyou County SGMA planning grants, with funding from California water bonds.

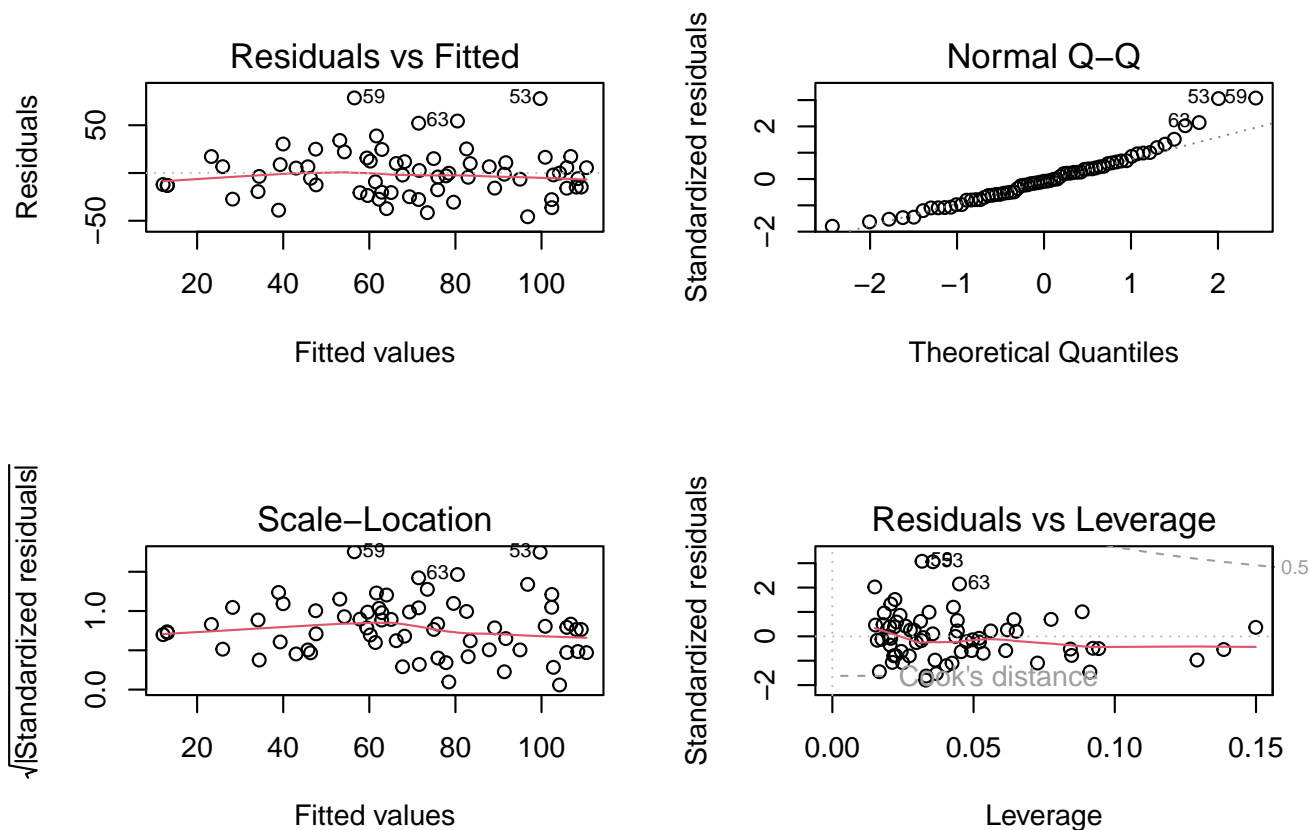


Figure A10. Diagnostic plots for the selected predictive models of P spill.

References

- Bunn, S. E. and Arthington, A. H.: Basic principles and ecological consequences of altered flow regimes for aquatic biodiversity, *Environmental Management*, 30, 492–507, <https://doi.org/10.1007/s00267-002-2737-0>, 2002.
- 570 Burnham, K. P. and Anderson, D. R.: *Multimodel inference: A Practical Information-Theoretic Approach*, 2004.
- California Department of Fish and Wildlife (CDFW): Cooperative Report of the Scott River Coho Salmon Rescue and Relocation Effort: 2014 Drought Emergency, Tech. Rep. August, California Department of Fish and Wildlife (CDFW), <https://www.fs.usda.gov/Internet/FSE{ }DOCUMENTS/stelprd3850544.pdf>, 2015.
- California Department of Water Resources (DWR): Bulletin 118: Scott River Valley Groundwater Basin, Tech. rep., <https://water.ca.gov/LegacyFiles/pubs/groundwater/bulletin{ }118/basindescriptions/1-5.pdf>, 2004.
- 575 California Department of Water Resources (DWR): Sustainable Groundwater Management Act - Water Year Type Dataset Development Report, Tech. Rep. January, Department of Water Resources - Sustainable Groundwater Management Office, 2021.

California Department of Water Resources (DWR): Notice to State Water Project Contractors: 2022 State Water Project Table A Allocation Decrease from 15 to 5 Percent, <https://water.ca.gov/-/media/DWR-Website/Web-Pages/Programs/State-Water-Project/Management/SWP-Water-Contractors/Files/22-03-2022-SWP-Allocation-Decrease-5-Percent-031822.pdf>, 2022.

California Department of Water Resources (DWR): State Water Project, <https://water.ca.gov/programs/state-water-project>, 2023.

Colorado Division of Water Resources: Drought & Surface Water Supply Index, <https://dwr.colorado.gov/services/water-administration/drought-and-swsi>, 2023.

Foglia, L., McNally, A., Hall, C., Ledesma, L., Hines, R., and Harter, T.: Scott Valley Integrated Hydrologic Model : Data Collection , Analysis , and Water Budget, Tech. Rep. April, University of California, Davis, <http://groundwater.ucdavis.edu/files/165395.pdf>, 2013a.

Foglia, L., McNally, A., and Harter, T.: Coupling a spatiotemporally distributed soil water budget with stream-depletion functions to inform stakeholder-driven management of groundwater-dependent ecosystems, *Water Resources Research*, 49, 7292–7310, <https://doi.org/10.1002/wrcr.20555>, 2013b.

Foglia, L., Neumann, J., Tolley, D. G., Orloff, S. B., Snyder, R. L., and Harter, T.: Modeling guides groundwater management in a basin with river–aquifer interactions, *California Agriculture*, 72, 84–95, 2018.

Francis, R. C., Hare, S. R., Hollowed, A. B., and Wooster, W. S.: Effects of interdecadal climate variability on the oceanic ecosystems of the NE Pacific, *Fisheries Oceanography*, 7, 1–21, 1998.

Garen, D. C.: REVISED SURFACE-WATER SUPPLY INDEX FOR WESTERN UNITED STATES, *Journal of Water Resources Planning and Management*, 119, 437–454, <https://water.ca.gov/-/media/DWR-Website/Web-Pages/Programs/State-Water-Project/Management/SWP-Water-Contractors/Files/22-03-2022-SWP-Allocation-Decrease-5-Percent-031822.pdf>, 1993.

Gorman, M. P.: Juvenile survival and adult return as a functional of freshwater rearing life history for coho salmon in the Klamath River basin, Master’s thesis, Humboldt State University, <https://digitalcommons.humboldt.edu/cgi/viewcontent.cgi?article=1005{&}context=etd>, 2016.

Guttman, N. B.: COMPARING THE PALMER DROUGHT INDEX AND THE STANDARDIZED PRECIPITATION INDEX ’ ties of the PDSI and its variations have been the referenced studies show that the intended, *Journal Of The American Water Resources Association*, 34, 113–121, <https://doi.org/10.1111/j.1752-1688.1998.tb05964.x>, 1998.

Harter, T. and Hines, R.: Scott Valley Community Groundwater Study Plan, Tech. rep., Groundwater Cooperative Extension Program University of California, Davis, Davis, CA, <http://groundwater.ucdavis.edu/files/136426.pdf>, 2008.

James, G., Witten, D., Hastie, T., and Tibshirani, R.: *An Introduction to Statistical Learning*, Springer Science+Business Media, New York, 7th edn., <https://doi.org/10.1007/978-1-4614-7138-7>, 2013.

Mack, S.: *Geology and Ground-Water Features of Scott Valley Siskiyou County, California.*, Tech. rep., Geological Survey Water-Supply Paper 1462, <https://pubs.usgs.gov/wsp/1462/report.pdf>, 1958.

Mahoney, J. M. and Rood, S. B.: Streamflow requirements for cottonwood seedling recruitment-An integrative model, *Wetlands*, 18, 634–645, <https://doi.org/10.1007/BF03161678>, 1998.

McDonnell, J. J., Spence, C., Karran, D. J., van Meerveld, H. J., and Harman, C. J.: Fill-and-Spill: A Process Description of Runoff Generation at the Scale of the Beholder, *Water Resources Research*, 57, 1–13, <https://doi.org/10.1029/2020WR027514>, 2021.

McKee, T. B., Doesken, N. J., and Kleist, J.: The relationship of drought frequency and duration to time scales, in: *Proceedings of the Eighth Conference on Applied Climatology*, January, p. 5, Anaheim, California, 1993.

Moyle, P.: Coho Salmon, *Oncorhynchus kisutch* (Walbaum), in: *Inland Fishes of California*, pp. 245–251, 2002.

- 615 Natural Resources Conservation Service (NRCS): Idaho Water Supply Outlook Report, Tech. rep., USDA, Boise, ID, <https://www.wcc.nrcs.usda.gov/ftpref/support/states/ID/wy2023/wsor/borid623.pdf>, 2023.
- Null, S. E. and Viers, J. H.: In bad waters: Water year classification in nonstationary climates, *Water Resources Research*, 49, 1137–1148, <https://doi.org/10.1002/wrcr.20097>, 2013.
- Palmer, W. C.: Meteorological Drought, Research Paper No. 45, Tech. rep., US Weather Bureau, Washington, D.C., 1965.
- 620 Patterson, N. K., Lane, B. A., Yarnell, S. M., Qiu, Y., Sandoval-Solis, S., and Pasternack, G. B.: A hydrologic feature detection algorithm to quantify seasonal components of flow regimes, *Journal of Hydrology*, 585, 2020.
- Peek, R., Irving, K., Yarnell, S. M., Lusardi, R., Stein, E. D., and Mazor, R.: Identifying Functional Flow Linkages Between Stream Alteration and Biological Stream Condition Indices Across California, *Frontiers in Environmental Science*, 9, 1–14, <https://doi.org/10.3389/fenvs.2021.790667>, 2022.
- 625 Poff, N. L., Allan, J. D., Bain, M. B., Karr, J. R., Prestegard, K. L., Richter, B. D., Sparks, R. E., and Stromberg, J. C.: A paradigm for river conservation and restoration, *BioScience*, 47, 769–784, <https://doi.org/10.2307/1313099>, 1997.
- Poff, N. L., Richter, B. D., Arthington, A. H., Bunn, S. E., Naiman, R. J., Kendy, E., Acreman, M., Apse, C., Bledsoe, B. P., Freeman, M. C., Henriksen, J., Jacobson, R. B., Kennen, J. G., Merritt, D. M., O’Keeffe, J. H., Olden, J. D., Rogers, K., Tharme, R. E., and Warner, A.: The ecological limits of hydrologic alteration (ELOHA): A new framework for developing regional environmental flow standards, *Freshwater*
- 630 *Biology*, 55, 147–170, <https://doi.org/10.1111/j.1365-2427.2009.02204.x>, 2010.
- Pyschik, J.: Assessing Climate Impacts Against Groundwater Pumping Impacts on Stream Flow with Statistical Analysis, Master’s, Albert Ludwigs University Freiburg, 2022.
- Scott River Water Trust (SRWT): 2017 Monitoring Report, Tech. Rep. June, <https://www.scottwatertrust.org/blank>, 2018.
- Siskiyou County Flood Control and Water Conservation District: Scott Valley Groundwater Sustainability Plan, Tech. rep., Siskiyou County
- 635 Flood Control and Water Conservation District, <https://www.co.siskiyou.ca.us/naturalresources/page/scott-valley-gsp-chapters>, 2021.
- Sommarstrom, S.: Email communication regarding connectivity of Scott River tailings reach, Nov. 18, 2020, 2020.
- Tarboton, D. G.: Rainfall-Runoff Processes., <http://www.engineering.usu.edu/dtarb/rrp.html>, 2003.
- Tolley, D. G., Foglia, L., and Harter, T.: Sensitivity Analysis and Calibration of an Integrated Hydrologic Model in an Irrigated Agricultural Basin with a Groundwater-Dependent Ecosystem, *Water Resources Research*, 55, <https://doi.org/10.1029/2018WR024209>, 2019.
- 640 Tromp-Van Meerveld, H. J. and McDonnell, J. J.: Threshold relations in subsurface stormflow: 2. The fill and spill hypothesis, *Water Resources Research*, 42, 1–11, <https://doi.org/10.1029/2004WR003800>, 2006.
- Van Kirk, R. W. and Naman, S. W.: Relative effects of climate and water use on base-flow trends in the lower Klamath Basin, *Journal of the American Water Resources Association*, 44, 1035–1052, <https://doi.org/10.1111/j.1752-1688.2008.00212.x>, 2008.
- Verley, F.: Lessons from Twenty Years of Local Volumetric Groundwater Management: The Case of the Beauce Aquifer, Central France, in:
- 645 *Sustainable Groundwater Management: A Comparative Analysis of French and Australian Policies and Implications to Other Countries*, edited by Rinaudo, J.-D., Holley, C., Barnett, S., and Montginoul, M., pp. 93–108, Springer Nature Switzerland AG, Cham, Switzerland, <https://doi.org/10.1142/s2382624x22800017>, 2020.
- Wheeler, K., Wenger, S. J., and Freeman, M. C.: States and rates: Complementary approaches to developing flow-ecology relationships, *Freshwater Biology*, 63, 906–916, <https://doi.org/10.1111/fwb.13001>, 2018.
- 650 Wilhite, D. A. and Glantz, M. H.: Understanding: The drought phenomenon: The role of definitions, *Water International*, 10, 111–120, <https://doi.org/10.1080/02508068508686328>, 1985.

- Wilhite, D. A., Hayes, M. J., and Svoboda, M.: Drought Monitoring and Assessment : Status and Trends in the United States, Drought Mitigation Center Faculty Publications, 76, <http://digitalcommons.unl.edu/droughtfacpub/76>, 2000.
- Williams, A., Cook, E., Smerdon, J., Cook, B., Abatzoglou, J., Bolles, K., Baek, S., Badger, A., and Livne, B.: Large contribution from anthropogenic warming to an emerging North American megadrought, *Science*, In press, 314–318, 2020.
- Yarnell, S. M., Stein, E. D., Webb, J. A., Grantham, T., Lusardi, R. A., Zimmerman, J., Peek, R. A., Lane, B. A., Howard, J., and Sandoval-Solis, S.: A functional flows approach to selecting ecologically relevant flow metrics for environmental flow applications, *River Research and Applications*, 36, 318–324, <https://doi.org/10.1002/rra.3575>, 2020.